

The Limit of Mechanical Stability in Quantum Solids: A Diffusion Monte Carlo Study

Claudio Cazorla¹ and Jordi Boronat²

¹*Institut de Ciència de Materials de Barcelona (ICMAB-CSIC), 08193 Bellaterra, Spain*

²*Departament de Física i Enginyeria Nuclear, Universitat Politècnica de Catalunya, Campus Nord B4-B5, E-08034, Barcelona, Spain**

We present a first-principles study of the energy and elastic properties of solid helium at pressures below the range in which is energetically stable. We find that the limit of mechanical stability in hcp ⁴He is $P_s = -33.82$ bar, which lies significantly below the spinodal pressure found in the liquid phase (i.e., -9.6 bar). Furthermore, we show that the pressure variation of the transverse and longitudinal sound velocities close to P_s do not follow a power law of the form $\propto (P - P_s)^\gamma$, in contrast to what is observed on the fluid.

PACS numbers: 67.80.-s, 02.70.Ss, 67.40.-w

I. INTRODUCTION

In the last two decades, extensive theoretical and experimental works have focused on the study of liquid helium at negative pressures and ultra-low temperatures.^{1,2} The equation of state of this material has been measured very accurately within the density range in which is stable, and extrapolated to the region of negative pressures.^{3,4} On the theoretical side, quantum Monte Carlo methods have allowed for precise and explicit simulation of metastable liquid helium, producing results which are in remarkable good agreement with experiments.⁵ A quantity of central interest in all these studies is the spinodal point P_s , i.e., the pressure at which the bulk modulus, B , and sound velocity go to zero and thus the liquid becomes unstable against long wavelength density fluctuations. In liquid ⁴He P_s amounts to -9.6 bar, while in liquid ³He to -3.2 bar.

Analogous studies performed in solid helium are almost non-existent in the literature.^{6,7} At $T = 0$ K solid helium becomes stable at pressures larger than ~ 25 bar thus certainly the realm of negative pressures lies well below such a threshold. Nevertheless, analysis of the mechanical instability limit in helium crystals turns out to be a topic of fundamental interest. In contrast to liquids, solids can sustain shear stresses and because of this ordinary fact the definition of the spinodal density in crystals differs significantly from the one given above. In the particular case of solid ⁴He, previous attempts at determining P_s have been, to the best of our knowledge, only tentative.^{6,7}

The energy of a crystal under a homogeneous elastic deformation is

$$E(V, \eta) = E_0(V) + \frac{1}{2}V \sum_{ij} C_{ij} \eta_i \eta_j, \quad (1)$$

where $\{C_{ij}\}$ are the elastic constants and $\{\eta_i\}$ a general strain deformation (both expressed in Voigt notation). The specific symmetry of a crystal determines the number of independent elastic constants which are different from zero. In the case of hexagonal crystals (e.g., hcp ⁴He) these are five: C_{11} , C_{12} , C_{13} , C_{33} and C_{44} . The con-

ditions for mechanical stability in a crystal follow from the requirement that upon a general strain deformation the change in the total energy must be positive. It can be shown that in hcp crystals subjected to an external pressure P , these conditions readily are^{8,9}

$$\begin{aligned} C_{44} - P &> 0 \quad [\text{C1}] \\ C_{11} - C_{12} - 2P &> 0 \quad [\text{C2}] \\ (C_{33} - P)(C_{11} + C_{12}) - 2(C_{13} + P)^2 &> 0 \quad [\text{C3}]. \quad (2) \end{aligned}$$

The spinodal pressure, or limit of mechanical stability, in a crystal then is identified with the point at which any of the three conditions above is not fulfilled. We must note that the bulk modulus of an hexagonal crystal can be expressed as¹⁰

$$B = -V \frac{dP}{dV} = \frac{C_{33}(C_{11} + C_{12}) - 2C_{13}^2}{C_{11} + C_{12} + 2C_{33} - 4C_{13}}, \quad (3)$$

thus the conditions at which the bulk modulus (and sound velocities) vanishes in general must not coincide with the corresponding limit of mechanical stability. This reasoning is in fact different from the usual P_s analysis performed in liquids.

In this article we present a computational study of the energetic and elastic properties in solid ⁴He at pressures below ~ 25 bar, based on the diffusion Monte Carlo method. Our first-principles calculations allow us to determine with rigor and precision the limit of mechanical stability in this material, which we estimate to be $P_s = -33.82$ bar (that is, much larger in absolute value than the one found in the fluid). Moreover, we show that, in contrast to liquid helium, the pressure variation of the sound velocities near P_s do not follow a power law of the form $\propto (P - P_s)^\gamma$ with $\gamma = 1/3$.¹¹

The organization of this article is as follows. In the next section, we provide the details of our computational method and calculations. In Sec. III, we present our results and comment on them. Finally, we summarize our main findings in Sec. IV.

II. COMPUTATIONAL DETAILS

In DMC the time-dependent Schrödinger equation of a N -particle system is solved stochastically by simulating the time evolution of the Green's function propagator $e^{-\frac{i}{\hbar}\hat{H}t}$ in imaginary time $\tau \equiv \frac{it}{\hbar}$. In the $\tau \rightarrow \infty$ limit, sets of configurations (walkers) $\{\mathbf{R}_i \equiv \mathbf{r}_1, \dots, \mathbf{r}_N\}$ render the probability distribution function $\Psi_0\Psi$, where Ψ_0 is the true ground-state wave function and Ψ a guiding wave function used for importance sampling. Within DMC, virtually exact results (i.e., subjected to statistical uncertainties only) can be obtained for the ground-state energy and related quantities.^{12,13}

We are interested in studying the ground-state of hcp ${}^4\text{He}$, which we assume to be governed by the Hamiltonian $H = -\frac{\hbar^2}{2m_{\text{He}}} \sum_{i=1}^N \nabla_i^2 + \sum_{i<j}^N V_{\text{He-He}}(r_{ij})$ where m_{He} is the mass of a ${}^4\text{He}$ atom and $V_{\text{He-He}}$ the semi-empirical pairwise potential due to Aziz.¹⁴ It is worth noticing that the Aziz potential provides an excellent description of the He-He interactions at low pressure.^{15,16}

The guiding wave function that we use in this study, Ψ_{SNJ} , reproduces both the crystal ordering and Bose-Einstein symmetry. This model wave function was introduced in Ref. [17] and reads

$$\Psi_{\text{SNJ}}(\mathbf{r}_1, \dots, \mathbf{r}_N) = \prod_{i<j}^N f(r_{ij}) \prod_{J=1}^N \left(\sum_{i=1}^N g(r_{iJ}) \right), \quad (4)$$

where the index in the second product runs over the lattice position vectors. In previous works we have demonstrated that Ψ_{SNJ} provides an excellent description of the ground-state properties of bulk hcp ${}^4\text{He}$ ¹⁷ and quantum solid films.¹⁸⁻²⁰ Here, we adopt the correlation functions in Eq. (4) of the McMillan, $f(r) = \exp[-1/2 (b/r)^5]$, and Gaussian, $g(r) = \exp[-1/2 (ar^2)]$, forms, and optimize the corresponding parameters with variational Monte Carlo.

The technical parameters in our calculations were set in order to ensure convergence of the total energy per particle to less than 0.02 K/atom. The value of the mean population of walkers was 500 and the length of the imaginary time-step ($\Delta\tau$) $5 \cdot 10^{-4} \text{ K}^{-1}$. We used large simulation boxes containing 200 atoms in all the cases. Statistics were accumulated over 10^5 DMC steps performed after system equilibration, and the approximation used for the short-time Green's function $e^{-\hat{H}\tau}$ is exact up to third order in τ .^{21,22}

The computational strategy that we followed for calculation of the elastic constants $\{C_{ij}\}$ is the same than explained in works [10,23,24], thus we address the interested reader to them.

III. RESULTS AND DISCUSSION

In Fig. 1, we show the calculated energy in solid helium expressed as a function of volume (solid symbols). We

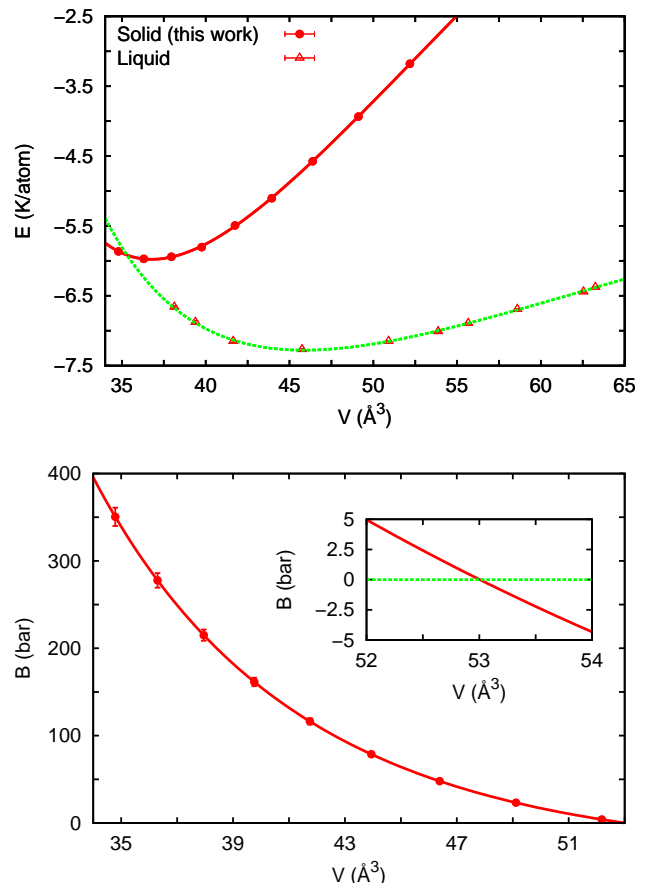


FIG. 1: (Top:) Calculated energy per particle expressed as a function of volume. The solid line represents a polynomial fit to our results (see text). Results obtained in the liquid phase (from work [5]) are shown for comparison. (Bottom:) Calculated bulk modulus expressed as a function of volume. The region in which B vanishes is augmented on the inset.

fitted our results to the polynomial curve

$$E(V) = E_0 + b \left[\left(\frac{V_0}{V} \right) - 1 \right]^2 + c \left[\left(\frac{V_0}{V} \right) - 1 \right]^3, \quad (5)$$

and found as best parameters $E_0 = -5.978(5) \text{ K}$, $V_0 = 36.90(5) \text{ \AA}^3$, $b = 34.38(5) \text{ K}$, and $c = 7.86(5) \text{ K}$. In comparison to the analogous energy curve calculated in liquid helium (see Fig. 1),⁵ $E(V)$ displays larger slopes, which translates into larger negative pressures, at volumes close to equilibrium (i.e., V_0). In the same figure, we enclose the bulk modulus, $B(V) = Vd^2E/dV^2$, that is calculated directly from $E(V)$ (solid line). The symbols which appear therein correspond to estimations obtained with Eq.(3), thereby excellent consistency between our energy and C_{ij} calculations is demonstrated. We find that the bulk modulus of helium vanishes at $V_B = 53.00 \text{ \AA}^3$ and $P_B = -34.06 \text{ bar}$. In what follows, we present our analysis of the elastic properties and mechanical stability in solid ${}^4\text{He}$ and clarify whether V_B and P_B are meaningful

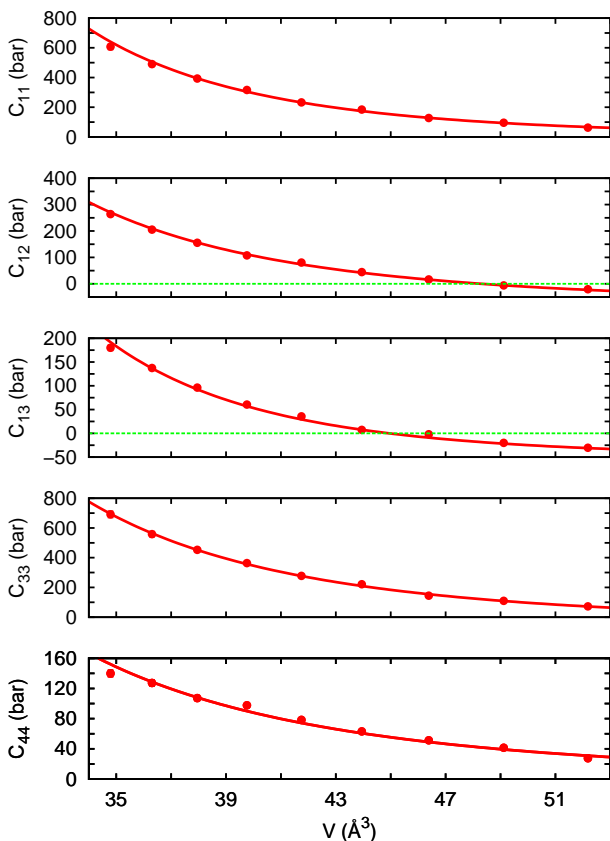


FIG. 2: Calculated elastic constants expressed as a function of volume. The solid lines are power-law fits to our results (solid symbols).

physical quantities.

Fig. 2 shows how the calculated elastic constants in solid helium change as a function of volume. As it is appreciated therein, all five C_{ij} decrease with increasing volume. In particular, C_{12} and C_{13} become zero at $V = 48.32$ ($P = -32.80$ bar) and 44.95 \AA^3 (-29.47 bar) respectively. We performed power-law fits to our $C_{ij}(V)$ results in order to render continuous elastic constant functions. By doing this, we were able to represent the three conditions of mechanical stability in hcp helium [see Eq.(2)] as a function of volume. These results are enclosed in Fig. 3 and it is observed there that condition 3 in Eq.(2) [C3], is violated at $V_s = 50.81 \text{ \AA}^3$ and $P_s = -33.82$ bar. Thus, we identify the (V_s, P_s) point with the limit of mechanical stability in solid ^4He . These conditions are not coincident with the (V_B, P_B) state at which the bulk modulus vanishes, as in fact was already expected from Eqs.(2)-(3).

Sound velocities in solids can be either longitudinal or tranverse and depend on the direction of propagation. In crystals with hexagonal symmetry two main propagation modes are identified, one along the c -axis and the other contained in the basal plane. The relationships between the elastic constants and sound velocities in hcp crystals are¹⁰

$$\begin{aligned} v_L &= (C_{33}/\rho)^{1/2} \\ v_{T1} = v_{T2} &= (C_{44}/\rho)^{1/2} \end{aligned} \quad (6)$$

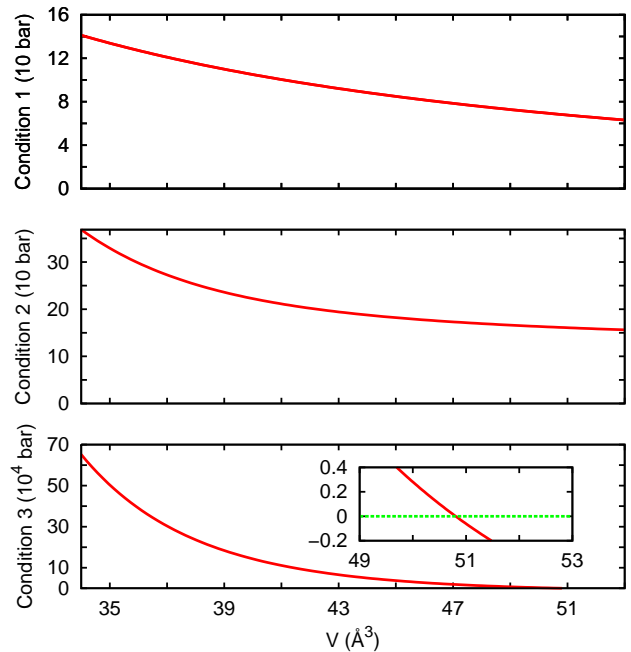


FIG. 3: Conditions of mechanical stability [see Eq.(2)] expressed as a function of volume. The region in which condition 3 is not accomplished is augmented on the inset.

along the c -axis, and

$$\begin{aligned} v_L &= (C_{11}/\rho)^{1/2} \\ v_{T1} = (C_{11} - C_{12}/2\rho)^{1/2} \quad v_{T2} &= (C_{44}/\rho)^{1/2} \end{aligned} \quad (7)$$

in the basal plane. In Fig. 4, we plot the six sound velocities calculated in solid helium as a function of pressure (some of them are coincident) together with an appropriate average of them, v_D .¹⁰ We observe that none of the sound velocities vanishes at the spinodal pressure P_s (marked in red in the figure), as it was already expected from Eqs.(2)-(6)-(7). Neither any sound velocity becomes zero at P_B , the pressure at which the bulk modulus vanishes. These results indeed are totally different from the usual conclusions drawn on the mechanical stability of liquids.

Recently, it has been suggested that the variation of the sound velocities near the spinodal density in solid ^4He could follow a power law of the form $\propto (P - P_s)^\gamma$ where $\gamma = 1/3$, in analogy to what is observed on the liquid.^{6,7} However, in light of the results enclosed in Fig. 4 such an hypotheses can not be valid since none of the sound velocities becomes zero at P_s . Furthermore, we performed fits of the form $v_{L,T}(P) = a + b(P - P_s)^\beta$ to our results and found that parameter β was never equal to $1/3$ and depended on the considered velocity. Therefore, we must conclude that the propagation of sound waves in helium crystals at the verge of mechanical instability differs radically from that in liquid helium under similar conditions.

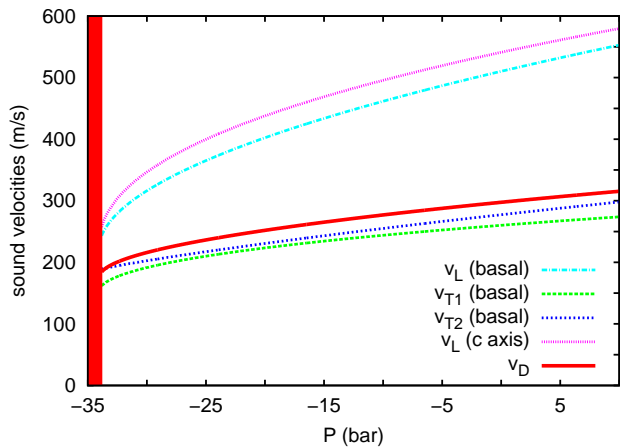


FIG. 4: Calculated sound velocities along the c -axis and in the basal plane [see Eqs.(6)-(7)] expressed as a function of pressure. The region in which the crystal becomes mechanically unstable is filled with red color.

IV. CONCLUSIONS

We have presented a rigorous and precise computational study of the energy and elastic properties of solid helium at conditions in which is metastable. We have determined the limit of mechanical stability in this crystal, i.e., $P_s = -33.82$ bar, and the variation of the sound velocities at pressures close to it. Overall, we demonstrate that solid and liquid helium behave radically different in the vicinity of their spinodal points.

Acknowledgments

This work was supported by MICINN-Spain [Grants No. MAT2010-18113, CSD2007-00041, FIS2011-25275, and CSIC JAE-DOC program (C.C.)], and Generalitat de Catalunya [Grant No. 2009SGR-1003].

-
- * Electronic address: ccazorla@icmab.es
- ¹ J. A. Nissen, E. Bodegom, L. C. Brodie, J. S. Semura, Phys. Rev. B **40**, 6617 (1989).
 - ² H. J. Maris, S. Balibar, M. S. Pettersen, J. Low Temp. Phys. **93**, 1069 (1993).
 - ³ H. J. Maris, J. Low Temp. Phys. **98**, 403 (1995).
 - ⁴ H. J. Maris, D. O. Edwards, J. Low Temp. Phys. **129**, 1 (2002).
 - ⁵ J. Boronat, J. Casulleras, and J. Navarro, Phys. Rev. B **50**, 3427 (1994).
 - ⁶ H. J. Maris, J. Low Temp. Phys. **155**, 290 (2009).
 - ⁷ H. J. Maris, J. Low Temp. Phys. **158**, 485 (2010).
 - ⁸ G. V. Sin'ko and N. A. Smirnov, J. Phys.: Condens. Matter **14**, 6989 (2002).
 - ⁹ G. Grimvall *et al.*, Rev. Mod. Phys. **84**, 945 (2012).
 - ¹⁰ C. Cazorla, Y. Lutsyshyn, and J. Boronat, Phys. Rev. B **85**, 024101 (2012).
 - ¹¹ H. J. Maris, Phys. Rev. Lett. **66**, 45 (1991).
 - ¹² R. Barnett, P. Reynolds, and W. A. Lester Jr., J. Comput. Phys. **96**, 258 (1991).
 - ¹³ J. Casulleras and J. Boronat, Phys. Rev. B **52**, 3654 (1995).
 - ¹⁴ R. A. Aziz, F. R. W. McCourt, and C. C. K. Wong, Mol. Phys. **61**, 1487 (1987).
 - ¹⁵ J. Boronat and J. Casulleras, Phys. Rev. B **49**, 8920 (1994).
 - ¹⁶ C. Cazorla and J. Boronat, J. Phys.: Condens. Matter **20**, 015223 (2008).
 - ¹⁷ C. Cazorla, G. Astrakharchick, J. Casulleras, and J. Boronat, New Journal of Phys. **11**, 013047 (2009).
 - ¹⁸ C. Cazorla and J. Boronat, Phys. Rev. B **77**, 024310 (2008).
 - ¹⁹ C. Cazorla, G. Astrakharchick, J. Casulleras, and J. Boronat, J. Phys.: Condens. Matter **22**, 165402 (2010).
 - ²⁰ M. C. Gordillo, C. Cazorla, and J. Boronat, Phys. Rev. B **83**, 121406(R) (2011).
 - ²¹ J. Boronat and J. Casulleras, Phys. Rev. B **49**, 8920 (1994).
 - ²² S. A. Chin, Phys. Rev. A **42**, 6991 (1990).
 - ²³ C. Cazorla, Y. Lutsyshyn, and J. Boronat, Phys. Rev. B **87**, 214522 (2013).
 - ²⁴ R. Rota, Y. Lutsyshyn, C. Cazorla, and J. Boronat, J. Low Temp. Phys. **168**, 150 (2012).